Comparison of Activity Coefficient Models for Electrolyte Systems

Yi Lin
Haldor Topsøe A/S, Nymøllevej 55, 2800 Kgs. Lyngby, Denmark

Antoon ten Kate
Akzo Nobel Chemicals bv, P.O. Box 9300, 6800 SB Arnhem, The Netherlands

Miranda Mooijer
Shell Global Solutions (Malaysia) Sdn Bhd (342714-T) Level 19, Tower 2, Petronas Twin Towers, 50088 Kuala Lumpur, Malaysia

Javier Delgado
SQM Salar S.A., El Trovador 4285, Santiago, Chile

Philip Loldrup Fosbøl and Kaj Thomsen
DTU Chemical Engineering, Søltofts Plads 229, 2800 Kgs. Lyngby, Denmark

DOI 10.1002/aic.12040
Published online December 15, 2009 in Wiley InterScience (www.interscience.wiley.com).

Three activity coefficient models for electrolyte solutions were evaluated and compared. The activity coefficient models are: The electrolyte NRTL model (ElecNRTL) by Aspentech, the mixed solvent electrolyte model (MSE) by OLI Systems, and the Extended UNIQUAC model from the Technical University of Denmark (DTU). Test systems containing a single salt (NaCl), multiple salts, and mixed solvent aqueous electrolyte solutions were chosen. The performance of the activity coefficient models were compared regarding the accuracy of solid–liquid and vapor–liquid equilibrium calculations for the test systems. © 2009 American Institute of Chemical Engineers *AIChE J,* 56: 1334–1351, 2010

Keywords: thermodynamics/classical, simulation, process, crystallization (precipitation), aqueous solutions, phase equilibrium

Introduction

Electrolyte solutions are encountered in many natural and industrial processes. Phase equilibrium calculations for solutions containing electrolytes are gaining increasing importance and it is important to choose the most suitable thermodynamic model for such systems. We have compared the performances of various activity coefficient models for electrolyte solutions. Especially, the accuracy of vapor–liquid equilibrium and solid liquid equilibrium calculations in binary, ternary, and multicomponent electrolyte systems is compared.

A number of activity coefficient models for electrolyte solutions have been developed for calculating the thermodynamic properties of electrolyte solutions for engineering applications. Some examples from the 1970s and 1980s are Meissner's

Additional Supporting Information may be found in the online version of this article.

Correspondence concerning this article should be addressed to K. Thomsen at kth@kt.dtu.dk

© 2009 American Institute of Chemical Engineers

model,[1–3] Bromley's model,[4] and Pitzer's model.[5,6] All these models can be seen as empirical extensions of the Debye-Hückel law. Another group of models combine local composition activity coefficient models with the Debye-Hückel law or modifications of the Debye-Hückel law. The models we have compared in this study belong to this group.

The thermodynamic modeling of phase equilibrium and other properties of solutions with electrolytes is very challenging. There are, therefore, many factors to be considered in the choice of thermodynamic model. Even though a certain model appears to represent a limited set of data accurately it does not guarantee the quality of this model.

Model, Theory, and Software

Three thermodynamic models for electrolyte solutions considered to be state of the art are studied here:

1. The implementation of the ElecNRTL model of Chen et al.[7–9] by Aspentech in Aspen Plus engineering suite 2006, version 20.0.

2. The implementation of the OLI MSE model of Wang et al.[10,11] and Kosinski et al.[12] in the OLI stream analyzer program, version 2.0.57.

3. The Extended UNIQUAC model of Thomsen et al.[13,14] and Thomsen[15,16] in software developed at DTU Chemical Engineering.

The two first of these models are implemented in process simulators while the last model is implemented in an academic software package. For the industry, access to the models in process simulators is important.

Thermodynamic models for electrolyte solutions traditionally consist of one or more long-range (LR) terms taking the electrostatic interactions between ions into account and one or more short-range (SR) terms that take the ion dipole interactions and the nonelectrostatic interactions into account. An overview of the different terms used in the models studied is given in Table 1.

The ElecNRTL model

Chen et al.[17] first developed a local composition NRTL activity coefficient model for single, completely dissociated electrolytes in a single solvent. An additional Born term was later added[18] and the model was thereby extended to mixed solvent electrolyte systems.

The ElecNRTL model has been applied to represent solid–liquid equilibrium (SLE) of aqueous multicomponent electrolyte systems[19] and phase equilibria of mixed solvent electrolyte systems[20] in a wide temperature range. It is being used in the Aspen Plus flowsheet simulator and has received wide acceptance in industrial modeling of electrolyte systems.

The ElecNRTL model is in Aspen Plus combined with an equation of state to calculate vapor phase fugacities in VLE systems. The ElecNRTL model is represented by the following excess Gibbs free energy expression.

$$G^{\mathrm{E}} = G^{\mathrm{E}}_{\mathrm{NRTL}} + G^{\mathrm{E}}_{\mathrm{Born}} + G^{\mathrm{E}}_{\mathrm{PDH}} \tag{1}$$

$G^{\mathrm{E}}_{\mathrm{NRTL}}$ is the SR NRTL term modified for use with electrolytes, $G^{\mathrm{E}}_{\mathrm{Born}}$ is the Born term, and $G^{\mathrm{E}}_{\mathrm{PDH}}$ is the Pitzer Debye-Hückel term.

The NRTL term was modified compared to the original Renon and Prausnitz[21] NRTL model. The modification consisted of adding the like-ion repulsion assumption and a local electroneutrality assumption. The modified NRTL term is given by:

$$\begin{aligned}\frac{G^{\mathrm{E}}_{\mathrm{NRTL}}}{RT} = &\sum_m X_m \frac{\sum_j X_m G_{jm}\tau_{jm}}{\sum_k X_k G_{jk}} \\ &+ \sum_c X_c \sum_{a'} \frac{X_{a'}\sum_j G_{jc,a'c}\tau_{jc,a'c}}{\left(\sum_{a''} X_{a''}\right)\left(\sum_k X_k G_{kc,a'c}\right)} \\ &+ \sum_a X_a \sum_{c'} \frac{X_{c'}\sum_j G_{ja,c'a}\tau_{ja,c'a}}{\left(\sum_{c''} X_{c''}\right)\left(\sum_k X_k G_{ka,c'a}\right)}\end{aligned} \tag{2}$$

The three summations in Eq. 2 are over molecular species (index m), cations (index c), and anions (index a). In this

Table 1. Overview of the Activity Coefficient Models Considered in This Study

	ElecNRTL	OLI MSE	Extended UNIQUAC
Short-range term	The electrolyte NRTL model.	UNIQUAC model with quadratic temperature dependence.	UNIQUAC model with linear temperature dependence.
Long-range terms	1. Pitzer Debye-Hückel term. 2. Born term.	1. Pitzer Debye-Hückel term. 2. A second virial coefficient type term.	1. Extended Debye-Hückel term.
Model parameters	Two interaction parameters for each species pair.	Up to three interaction parameters for each species pair.	Volume and surface area parameter for each species. One interaction parameter per species pair.
Definition of species	Molecules and ion pairs	Molecules and ions	Molecules and ions
Determination of parameters	From binary and ternary data.	From binary and ternary data.	From binary and ternary data.
Solubility products/ equilibrium constants	From empirical correlation using up to four parameters per equilibrium.	From Helgeson-Kirkham-Flowers equation of state[25].	From tabulated standard state thermodynamic data[33].
Mixed solvent calculations	Gibbs energy of transfer. Composition dependence of relative permittivity	Gibbs energy of transfer. Composition dependence of relative permittivity	The non-ideality caused by the presence of other solvents is accounted for by the activity coefficient model.

Table 2. The Selected Test Systems Used in This Study

No.	System type	Components	Temperature (°C)	Source
A	Binary system	NaCl–H_2O	−21.9 to 110	Refs. 34,35,36,37,38,39, and various others
B	Binary system	Na_2SO_4-H_2O	25	Ref. 40 and various others
C	Ternary system	NaCl-$MgCl_2$-H_2O	0, 35	Ref. 41 and various others
D	Quaternary system	NaCl-KNO_3-H_2O	25	Refs. 42,43,44
E	Quaternary system	NaCl-K_2SO_4-H_2O	20	Refs. 45,46
F	Quaternary system	NaCl-$MgSO_4$-H_2O	35	Refs. 41,47
G	Quaternary system	NaCl-$MgNO_3$-H_2O	25	Ref. 48
H	Quinary system	NaCl-$MgSO_4$-$MgNO_3$-H_2O	0	Ref. 48
I	Quinary system	NaCl-$MgSO_4$-K_2SO_4-H_2O	55	Refs. 49,50,51
J	Ternary mixed solvent systems	NaCl-H_2O-Ethanol	15, 25	Refs. 52,53,54,55, and various others

equation, τ is calculated as a function of the binary, salt specific energy interaction parameters. $X_i = x_i C_i$. C_i is equal to the absolute value of the charge of an ion or equal to unity for a molecule. x_i is the mole fraction. $G_{ij} = \exp(-\alpha_{ij}\tau_{ij})$ with α_{ij} as the nonrandomness factor.

The Born term used in the ElecNRTL model is a modification of the Born expression of Robinson and Stokes.[22] The Born term accounts for the change of Gibbs free energy associated with moving ionic species from a mixed solvent state into an aqueous state.

The LR contribution is represented by the Pitzer-Debye-Hückel equation in form of the unsymmetrical, mole fraction based Pitzer-Debye-Hückel term.[23]

The adjustable parameters of the ElecNRTL model are the nonrandomness factors and the energy parameters of the local composition term. According to Mock et al.,[20] a system with two solvents and one salt requires nine adjustable binary parameters—at each temperature. The NRTL nonrandomness factors are often fixed in engineering practice which reduces the number of adjustable binary parameters required for such a system to six. Furthermore, up to four parameters can be used for each solid phase to calculate the solubility product as a function of temperature.

Aspen Plus offers a data regression system to allow users to determine the parameters of the elecNRTL model from available public or proprietary experimental data. According to the program manual, the program also provides built-in parameters for the electrolyte NRTL model. These parameters were developed using data for many industrially important electrolytic systems.

The OLI MSE model

In the OLI Systems software, the user can choose between the Bromley-Zemaitis aqueous model[24] and the OLI MSE (Mixed Solvent Electrolyte) model. The Bromley-Zemaitis model was previously the primary model in OLI Systems software. In this comparison project, the OLI MSE model was exclusively used as it represents the current technology from OLI.

The OLI MSE model is described by a three-term excess Gibbs energy function.[10–12]

$$G^E = G^E_{LR} + G^E_{SR} + G^E_{II} \tag{3}$$

The G^E_{LR} term represents the LR interactions caused by electrostatic forces. The contribution is expressed by the symmetric, mole fraction based Pitzer-Debye-Hückel expression.[23] The G^E_{SR} term accounts for the SR intermolecular interactions and is calculated by the UNIQUAC equation. The ionic interaction (II) term, G^E_{II} takes care of the specific ion–ion and ion–molecule interactions. It is calculated by an ionic strength-dependent symmetrical second viral coefficient type expression:

$$\frac{G^E_{II}}{RT} = -\left(\sum_i n_i\right)\sum_i\sum_j x_i x_j B_{ij}(I_x) \tag{4}$$

The summation is over all species $_i$ and $_j$. $B_{ij}(I_x) = B_{ji}(I_x)$, $B_{ii} = B_{jj} = 0$, and the ionic strength dependence of B_{ij} is given by

$$B_{ij}(I_x) = b_{ij} + c_{ij}\exp(-\sqrt{I_x + a_1}) \tag{5}$$

where b_{ij} and c_{ij} accounts for binary interaction. According to Gruszkiewicz et al.,[25] a_1 is set equal to 0.01. b_{ij} and c_{ij} are calculated as functions of temperature by

$$b_{ij} = b_{0,ij} + b_{1,ij}T + b_{2,ij}/T + b_{3,ij}T^2 + b_{4,ij}\ln T \tag{6}$$

$$c_{ij} = c_{0,ij} + c_{1,ij}T + c_{2,ij}/T + c_{3,ij}T^2 + c_{4,ij}\ln T \tag{7}$$

The last two parameters of Eqs. 6 and 7 are typically only necessary when there is a need to reproduce experimental

Table 3. Experimental and Calculated Values of the Bubble Point Pressure of Aqueous NaCl Solutions of Different Concentrations at 125°C

Experimental		Calculated Bubble Point Pressure (MPa)		
Molality (mol/kg H_2O)	Bubble P (MPa)	ElecNRTL	OLI MSE	Extended UNIQUAC
3.79	0.201	0.200	0.200	0.197
4.89	0.191	0.190	0.190	0.187
5.99	0.180	0.180	0.180	0.176
6.13	0.179	0.179	0.179	0.175
6.94	0.172	0.172	0.172	0.170
Average numerical difference		0.0004	0.0003	0.0034

The experimental data are from Liu and Lindsay.[37]

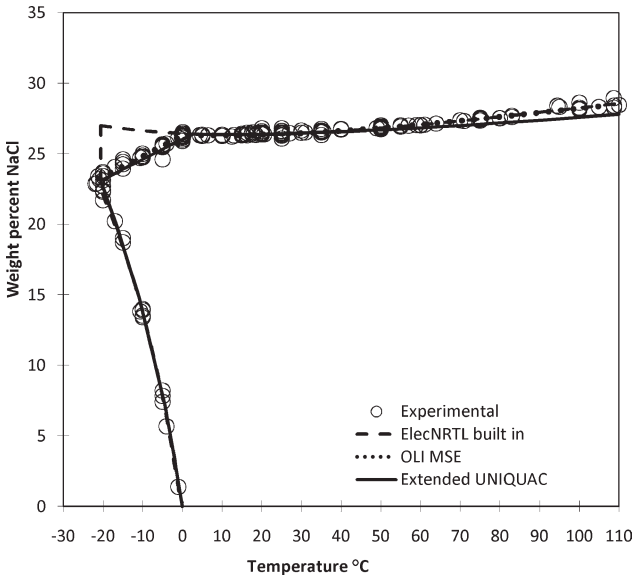

Figure 1. Solubility in the aqueous NaCl system as a function of temperature.

The circles mark experimental data from several sources as listed in Table 3.

data over a wide range of temperatures, e.g., from −50°C to 300°C. Otherwise, a more simple temperature dependence is used.

Standard state properties required for determining equilibrium constants and solubility products are obtained from the Helgeson-Kirkham-Flowers equation of state.[26]

For systems containing only strong electrolytes, the only model parameters required are in the II (ionic interaction) term. Some parameters for the OLI MSE model have been published.[10-12,25] The determination of parameters in the OLI MSE model is still a work in progress and the parameters might therefore be further improved in coming versions.

OLI Systems Inc. offers a data regression system in a separate program called Regress. The Regress program allows the user to determine or modify model parameters based on available published or proprietary experimental data.

The extended UNIQUAC model

The Extended UNIQUAC model is valid for multicomponent aqueous solutions of electrolytes and nonelectrolytes in industrially relevant temperature and pressure ranges. Thomsen et al.[13] first presented the Extended UNIQUAC model in its current form. It is an excess Gibbs free energy model consisting of three terms: An entropic term, $G^{E}_{\text{combinatorial}}$, an enthalpic term, G^{E}_{Residual}, and a Debye-Hückel electrostatic term, $G^{E}_{\text{Debye-Hiickel}}$:

$$G^{E} = G^{E}_{\text{combinatorial}} + G^{E}_{\text{Residual}} + G^{E}_{\text{Debye-Hiickel}} \tag{8}$$

The combinatorial and the residual terms are unchanged compared with the UNIQUAC model for nonelectrolytes. In the Extended UNIQUAC model, the same equations (Eqs. 8–12) are used for cations, anions, and for nonelectrolytes. The combinatorial term is given by

$$\frac{G^{E}_{\text{combinatorial}}}{RT} = \sum_i x_i \ln\left(\frac{\phi_i}{x_i}\right) - \frac{z}{2}\sum_i q_i x_i \ln\left(\frac{\phi_i}{\theta_i}\right) \tag{9}$$

$z = 10$ is the coordination number, x_i is the mole fraction, ϕ_i is the volume fraction and θ_i is the surface area fraction of component i. The residual term is given by

$$\frac{G^{E}_{\text{Residuial}}}{RT} = -\sum_i q_i x_i \ln\left(\sum_k \theta_k \psi_{ki}\right), \quad \text{where } \psi_{ki} = \exp\left(-\frac{u_{ki} - u_{ii}}{T}\right) \tag{10}$$

$u_{ki} = u_{ik}$ and u_{ii} are adjustable interaction parameters with linear temperature dependence. One of the strengths of the UNIQUAC model is that the excess Gibbs energy is modeled as an entropic term plus an enthalpic term. In comparison, the NRTL local composition model only contains an enthalpic term.

The Debye-Hückel term is expressed according to the unsymmetrical term suggested by Fowler and Guggenheim[27]:

$$\frac{G^{E}_{\text{Debye-Hiickel}}}{RT} = -x_w M_w \frac{4A}{b^3}\left[\ln(1 + bI^{1/2}) - bI^{1/2} + \frac{b^2 I}{2}\right] \tag{11}$$

I is the ionic strength, based on molality (mol/kg H_2O). In the Extended UNIQUAC model, molality is always calculated as mol of species per kg water. The parameter b is considered constant equal to 1.50 $(\text{kg/mol})^{[1/2]}$. The

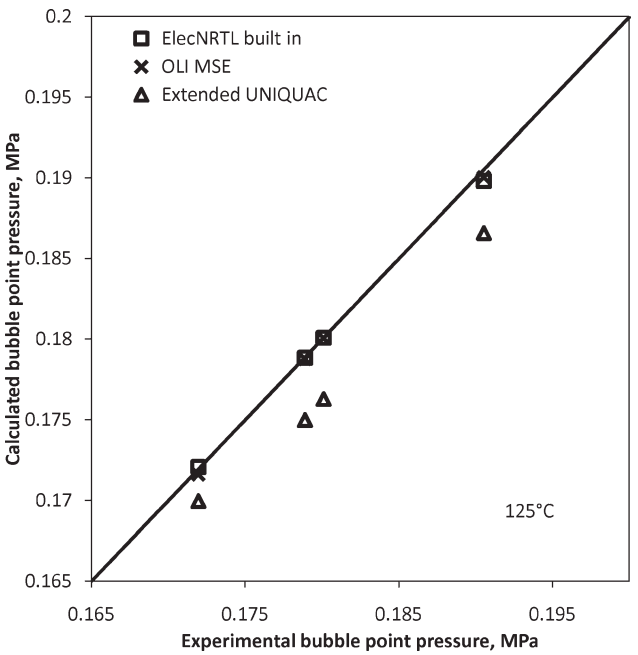

Figure 2. Parity plot for the bubble point pressure of aqueous NaCl solutions of different concentrations at 125°C.

The experimental data are from Liu and Lindsay.[37]

Table 4. Experimental and Calculated Values of the Bubble Point Pressure of Aqueous NaCl Solutions of Different Concentrations at 50°C

Experimental		Calculated Bubble point pressure (MPa)		
Molality (mol/kg H_2O)	Bubble P (MPa)	ElecNRTL	OLI MSE	Extended UNIQUAC
1.05	0.01192	0.01195	0.01192	0.01192
1.86	0.01156	0.01158	0.01155	0.01155
2.51	0.01125	0.01127	0.01124	0.01123
3.04	0.01100	0.01101	0.01098	0.01096
3.73	0.01065	0.01066	0.01063	0.01059
4.89	0.01002	0.01008	0.01002	0.00996
5.10	0.00990	0.00997	0.00991	0.00985
5.65	0.00960	0.00973	0.00962	0.00956
6.10	0.00934	0.00970	0.00937	0.00932
6.12	0.00933	0.00970	0.00936	0.00931
Average numerical difference		0.00011	0.00002	0.00003

The experimental data are from Gibbard et al.[38]

Debye-Hückel A parameter can be approximated in the temperature range 273.15 to 383.15 K according to Thomsen[15]:

$$A(T) = 1.131 + 1.335 \times 10^{-3} \times (T - 273.15) + 1.164 \times 10^{-5} \times (T - 273.15)^2 \ \mathrm{kg}^{1/2}/\mathrm{mol}^{1/2} \quad (15)$$

Thomsen and Rasmussen[14] combined the Extended UNIQUAC model with the Soave-Redlich-Kwong (SRK) EOS to calculate vapor–liquid equilibrium (VLE) in systems containing volatile components such as ammonia and carbon dioxide. Pereda et al.[28] applied the model to systems containing sulphur dioxide. It was shown by Iliuta et al.[29] and by Thomsen et al.[30] that the Extended UNIQUAC model is able to describe LLE (liquid–liquid equilibrium) and VLE in systems containing mixed solvents using the same set of parameters. This modeling was carried out by combining the original parameters developed for purely aqueous systems, with new parameters for alcohol–ion and alcohol–water interactions.

The Extended UNIQUAC model has also been applied in the study of mineral scale formation in geothermal and oilfield operations.[31,32] With the appropriate pressure parameters, the Extended UNIQUAC model is able to represent binary, ternary, and quaternary solubility data in the range of temperature and pressures from -20 to 250°C and 0.1 to 100 MPa, respectively.

Standard state properties such as Gibbs energy of formation, enthalpy of formation, and heat capacity of each species are used for calculating equilibrium constants as function of temperature. These standard state properties have mainly been obtained from tables published by NIST.[33] Property values that could not be found in these tables have been determined from experimental data.

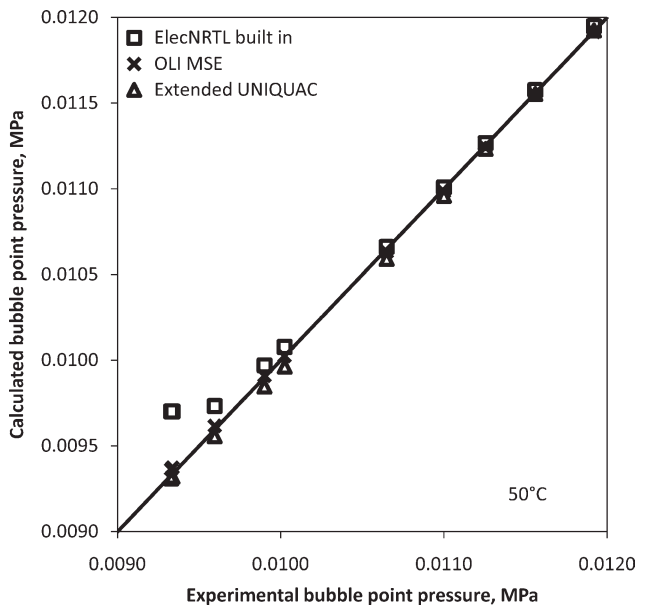

Figure 3. Parity plot of the bubble point pressure of aqueous NaCl solutions of different concentrations at 50°C.

The experimental data are from Gibbard et al.[38]

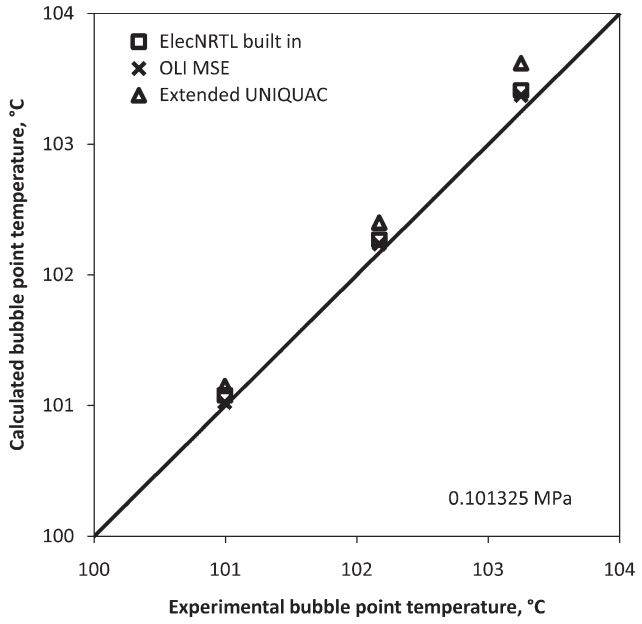

Figure 4. Parity plot for the bubble point temperature of aqueous NaCl solution of different concentrations at 0.101325 MPa.

The experimental data are from Hakuta et al.[39]

Table 5. Experimental and Calculated Values of the Bubble Point Temperatures of Aqueous NaCl Solutions of Different Concentrations at 0.101325 MPa

Experimental		Bubble point temperature (°C)		
Molality (mol/kg H_2O)	Bubble T (°C)	ElecNRTL	OLI MSE	Extended UNIQUAC
1.063	100.996	101.079	101.024	101.15
2.168	102.17	102.269	102.236	102.4
3.106	103.249	103.412	103.373	103.62
Average numerical difference		0.11	0.07	0.25

The experimental data are from Hakuta et al.[39]

Test systems for the electrolyte models

The three electrolyte models were tested on systems consisting of water, ethanol, Na^+, K^+, Mg^{2+}, Cl^-, NO_3^-, and SO_4^{2-}. The comparison was focused on subsystems containing NaCl except for one subsystem that concerns aqueous Na_2SO_4 solutions. The test systems are listed in Table 2. The accuracy of SLE calculations for binary, ternary, quaternary, and quinary salt systems including mixed solvent systems were studied, compared, and evaluated against experimental data. For some test systems VLE calculations were evaluated as well. In Tables 3 through 11, the experimental data used in the evaluation are presented together with the corresponding values calculated with the models. Average numerical differences between values calculated with each model and the corresponding experimental values are given in each table for easy comparison of performance. The quality of the experimental data used in this work is not discussed. The experimental data come from the open literature. The data were only used for comparing the performance of the different models, not for determining model parameters. The authors believe that the experimental data used here for the comparison of the models are the only data for the considered systems published in the open literature. The quality of the experimental data was not checked. In most cases the experimental data were measured and reported by different, independent research groups.

All the selected test systems are relatively simple systems. If more complicated systems such as partly dissociated systems were considered, the result might have been different.

Results and Discussion

Many built in parameters for the ElecNRTL model are delivered with the Aspen Plus program. These parameters do not cover all of the test systems shown in Table 2. For the comparison study here, C.-C. Chen from Aspentech, made several new parameter sets available for this project. Each parameter set is apparently optimized to give the best possible representation of each test system using the elecNRTL model. When these optimized parameters were used, the results are clearly labeled "ElecNRTL optimized". When the built in parameters were used, results are labeled "ElecNRTL built in." The parameter sets determined by C.-C. Chen can be obtained as Supporting Information from the website of this *Journal*.

Among the test systems listed in Table 2, parameters for all binary systems and the majority of ternary systems are

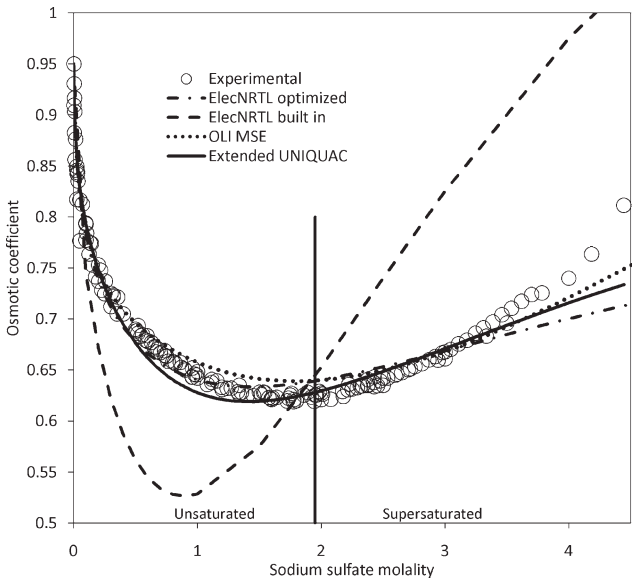

Figure 5. Osmotic coefficient of aqueous Na_2SO_4 solution of different concentrations at 25°C.

The vertical line indicates the saturated concentration of Na_2SO_4 (1.95 mol/kg) in water. The experimental data are from several sources including Robinson et al.[40]

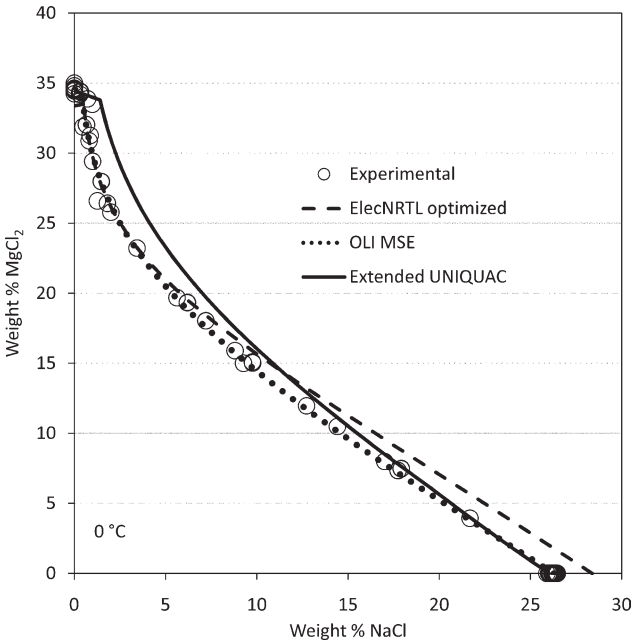

Figure 6. SLE phase diagram of the ternary aqueous system NaCl and $MgCl_2$ at 0°C.

Experimental data are from Autenrieth and Braune[41] and various others.

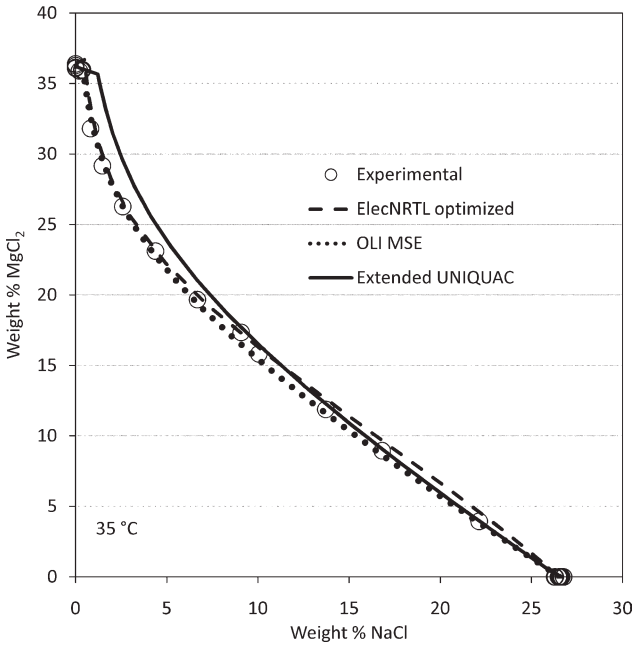

Figure 7. SLE phase diagram of the ternary aqueous system NaCl and $MgCl_2$ at 35°C.

Experimental data are from Autenrieth and Braune[41] and various others.

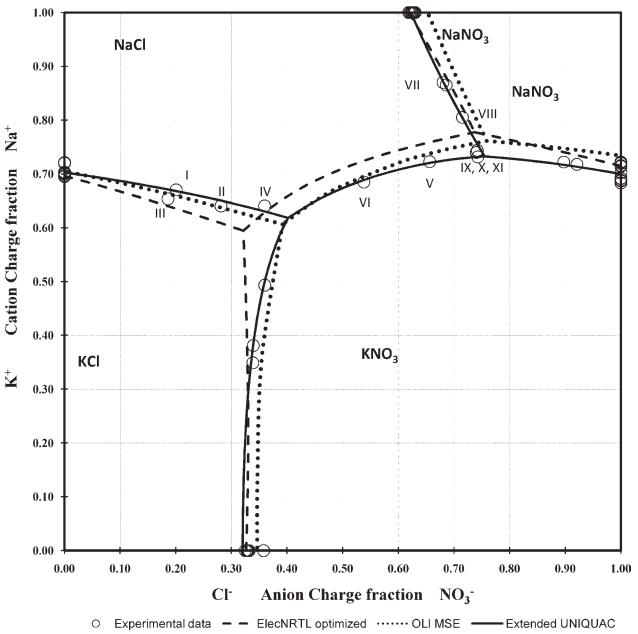

Figure 9. Quaternary phase diagram for the aqueous Na-K-Cl-NO_3 system at 25°C.

The experimental data are from Reinders,[42] Cornec and Krombach,[43] and Uyeda[44] and several others. The experimental data points chosen for the model comparison are marked with roman numerals and refer to the experimental compositions given in Table 7.

available for the OLI MSE model in the Stream Analyzer program, version 2.0.57. However, parameters for ternary systems containing $MgSO_4$ and/or K_2SO_4 are still incomplete. Therefore, calculations for systems V, VI, VIII, and IX are based on a partial coverage of parameters for the underlying ternary systems.

The model parameters for the three models were regressed from only binary and ternary data. In principle, the model parameters in a local composition model for electrolytes can be determined from binary and ternary data alone. When calculations are made for these binary and ternary systems, the results show how good the model *correlates* data. When calculations are performed for quaternary, quinary, or higher order systems, the results show how good the model is in *predicting* or *extrapolating* beyond the data type the parameters were fitted to.

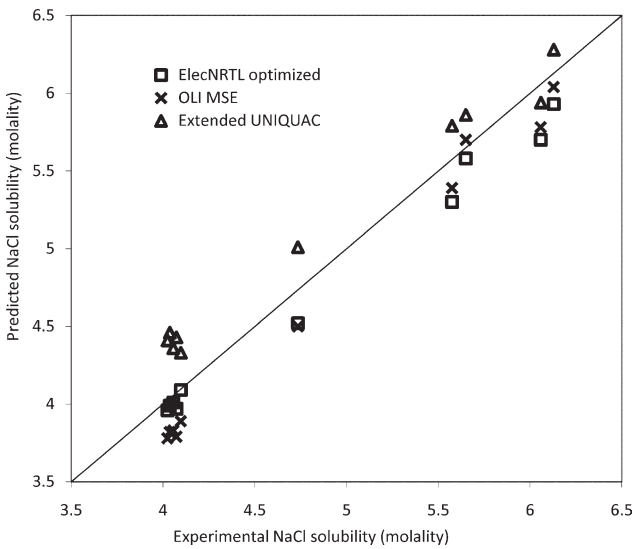

Figure 8. Parity plot for the NaCl solubility at 25°C in the aqueous Na-K-Cl-NO_3 system.

The experimental data are from Reinders,[42] Cornec and Krombach,[43] and Uyeda.[44]

Tetragene salts are salts like Kainite ($KCl \cdot MgSO_4 \cdot 3H_2O$) that consist of four different ions. To determine the standard state properties of tetragene salts, quaternary data are required because these salts can not precipitate from ternary solutions.

Computations concerning the 10 test systems with the three models, the ElecNRTL model, the OLI MSE model, and the Extended UNIQUAC model are compared regarding the following merits:

1 Accuracy of solid liquid equilibrium calculations for the selected test salt systems.

2 Freezing point depression (SLE)

3 Calculation of activity coefficients in super saturated solutions

4 Salt solubility/precipitation (SLE): saturation curve and stable salt form

5 Boiling point elevation (VLE) [unsaturated, saturated]

6 The performance of these models in mixed solvent systems.

Test system A: the NaCl-H_2O system

For the binary system NaCl-H_2O, the solubility diagram was calculated by the three models in the temperature range

Table 6. Results of the Model Comparison for the Aqueous System Na^+-K^+-Cl^--NO_3^- at 25°C

	Experimental NaCl solubility (mol/kg H_2O)					Calculated NaCl solubility (mol/kg H_2O)		
No.	KCl	$NaNO_3$	KNO_3	NaCl	Solid Phase*	ElecNRTL optimized NaCl	OLI MSE NaCl	Extended UNIQUAC NaCl
I	1.17		1.81	6.06	1	5.70	5.78	5.94 [1]
II	0.748		2.69	6.13	1	5.93	6.04	6.28 [1]
III	1.39		1.61	5.65	1	5.58	5.70 [1]	5.86 [1]
IV			3.99	7.10	1 + 2	6.34 [2]	6.48	6.78
V		5.22	3.81	4.73	2	4.52 [2]	4.50 [2]	5.01
VI		2.69	3.80	5.57	2	5.30 [2]	5.39 [2]	5.79
VII		7.19	1.76	4.10	3	4.09	3.89	4.33
VIII		7.40	2.78	4.06	3	4.01	3.83	4.36
IX		7.58	4.00	4.02	2 + 3	3.96 [2]	3.78 [2]	4.41 [2]
X		7.53	4.08	4.07	2 + 3	3.97 [2]	3.79 [2]	4.43
XI		7.44	4.21	4.04	2 + 3	3.99 [2]	3.82 [2]	4.46
Average numerical difference						0.19	0.24	0.27

The experimental compositions are given together with the NaCl solubility calculated with the models. All concentrations are in molality (mol/kg H_2O). The experimental data are from Reinders,[42] Cornec and Krombach,[43] and Uyeda.[44] The experimentally determined solid phases are given in column six. The solid phases determined by the models are given in brackets after the solubility. Roman numerals refer to the location of the data points in Figure 9.
*Solid phases in addition to NaCl are identified by 1 = KCl, 2 = KNO_3, 3 = $NaNO_3$.

from −22 to 110°C. The result is shown in Figure 1. At temperatures above 40°C, ElecNRTL and OLI provide better results than Extended UNIQUAC. The ElecNRTL does not predict the solubility curve for hydrohalite, $NaCl{\cdot}2H_2O$. This is the reason for the particular shape of the solubility curve calculated by ElecNRTL at low temperatures. Apparently, this salt is not included in the ElecNRTL model but has to be added and modeled by the user. The ice curve is calculated equally well by the three models.

Bubble Point Temperature and Pressure for NaCl-H_2O

Bubble point temperatures and pressures for aqueous NaCl solutions at different concentrations were calculated and compared with the corresponding experimental data. Parity plots were made for comparing the performance of the three models. Experimental data and calculated results for 125°C are presented in Table 3 where the concentration varies from 3.8 to 7 molal [18 to 29 wt %] NaCl. The calculation of bubble point pressures at this temperature is illustrated in the parity plot in Figure 2. The model parameters for the Extended UNIQUAC model were determined from data at temperatures up to 110°C.[13] The calculation therefore represents an extrapolation and some deviation is seen at 125°C for the Extended UNIQUAC model in Figure 2.

Calculations performed for NaCl solutions at 50°C are tabulated in Table 4 and shown in the parity plot in Figure 3. Apparently the models are better at reproducing the data for 50°C than 125°C, except for some deviation observed for the ElecNRTL model at low pressure and high concentrations.

Bubble point temperatures for dilute NaCl solutions at 1–3 molal [6–15 wt %] and 0.101325 MPa were calculated and compared with experimental data as illustrated in Figure 4 and Table 5. All three models gave satisfactory calculations of bubble point temperature and pressure.

Table 7. Results of the Model Comparison

	Experimental NaCl solubility (mol/kg H_2O)					Calculated NaCl solubility (mol/kg H_2O)		
No.	K_2SO_4	KCl	Na_2SO_4	NaCl	Solid Phases*	ElecNRTL optimized NaCl	OLI MSE NaCl	Extended UNIQUAC NaCl
I	0.239	1.57		5.33	1,2	6.82 [3]	5.49	5.51
II	0.239	1.57		5.34	1,2	6.82 [3]	5.48	5.50
III	0.266	1.49		5.42	1,2	6.88 [3]	5.52	5.55 [2]
IV	0.206	1.54		5.42	1,2	6.78 [3]	5.49	5.51
V	0.268	1.55		5.52	1,2	6.87 [3]	5.50	5.52 [2]
VI	0.511	0.410		5.82	2	7.54 [3]	6.07	6.09 [2]
VII	0.510		0.340	5.84	2,3	7.65 [3]	5.98	6.01
VIII	0.510		0.342	5.84	2,3	7.65 [3]	5.97	6.01
IX	0.511		0.339	5.85	2,3	7.65 [3]	5.98	6.01 [2]
X	0.520		0.340	5.94	3	7.67 [3]	5.98	6.01 [2]
XI	0.436			6.13	2	7.55 [3]	6.24	6.26
Average numerical difference						1.58	0.12	0.14

Experimental and predicted values of the solubility of NaCl in the aqueous Na^+-K^+-Cl^--SO_4^{2-} system at 20°C. The experimental data are from Teeple[45] and Bergman and Rustamov[46]. The experimentally determined solid phases are given in column six. The solid phases determined by the models are given in brackets after the solubility. Roman numerals refer to the location of the experimental data in Figure 10.
*Solid phases in addition to NaCl are identified by 1 = KCl, 2 = $NaK_3(SO_4)_2$, 3 = Na_2SO_4.

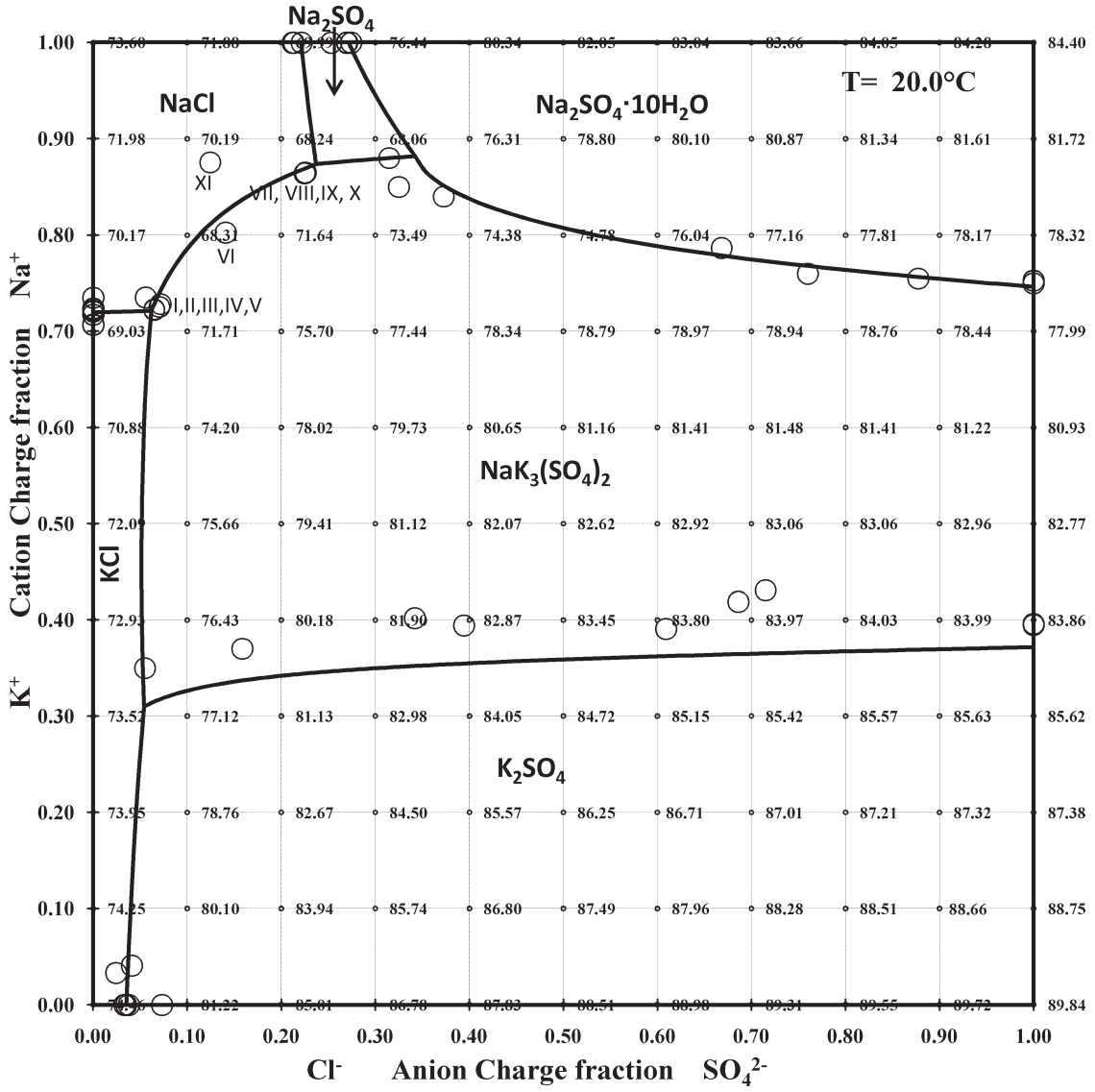

Figure 10. Quaternary phase diagram for the aqueous Na-K-Cl-SO_4 system at 20°C.

The black solid line is the prediction by Extended UNIQUAC. The water content predicted by the Extended UNIQUAC model is given in mass percent at grid intersections in the diagram. The experimental data are from Teeple[45] and Bergman and Rustamov.[46]

Test system B: osmotic coefficients for super saturated aqueous Na_2SO_4 solutions

Osmotic coefficients for aqueous Na_2SO_4 solutions at different concentrations were calculated and compared to experimental data. The comparison was performed into the super saturated region. The composition of saturation is marked with a vertical line in Figure 5.

The osmotic coefficient is defined as follows:

$$\Phi = \frac{n_{\text{solvent}} \ln a_{\text{solvent}}}{v n_{\text{solute}}} \tag{13}$$

n_{solvent} is the amount of solvent, n_{solute} is the amount of solute, and v is the number of ions produced from 1 mole of solute.

Experimental and calculated osmotic coefficients are plotted as function of molality (mol/kg H_2O) in Figure 5. The OLI MSE model and the Extended UNIQUAC model give slightly better results than the optimized ElecNRTL model. The built in ElecNRTL parameters give large deviations, even for dilute solutions.

Equation 13 shows how the osmotic coefficient is related to the water activity. The capability of the models to correlate osmotic coefficients is closely related to their potential to correlate the vapor pressure of water.

Test system C: NaCl-$MgCl_2$-H_2O at 0 and 35°C

The results of solubility calculations in the NaCl-$MgCl_2$-H_2O system are shown in Figures 6 and 7. For this ternary system, the ElecNRTL and OLI models provide better results than the Extended UNIQUAC model, especially at 0°C. The Extended UNIQUAC model parameters for the magnesium and calcium ions were not determined simultaneously with the parameters for the other ions.[13] These

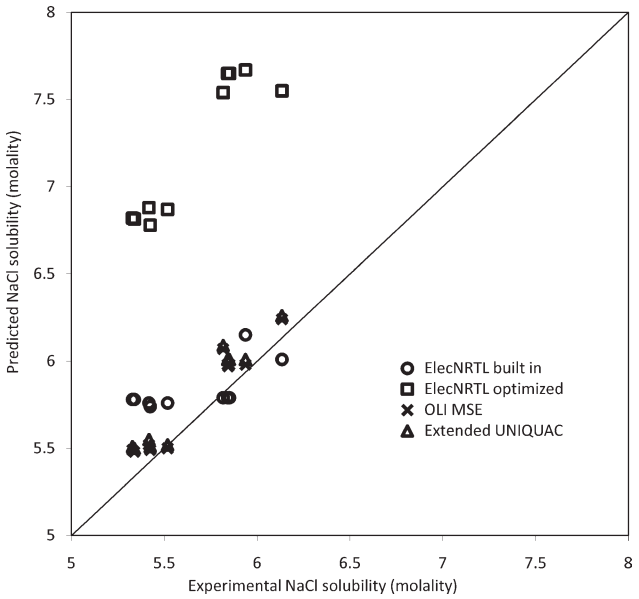

Figure 11. Parity plot for the NaCl solubility at 20°C in the aqueous Na-K-Cl-SO_4 system.

The experimental data are from Teeple[45] and Bergman and Rustamov.[46] The Aspen built in ElecNRTL parameters give a better result than the optimized ElecNRTL parameters.

parameters were later added to the model. This is believed to be the reason for the deviation.

Quaternary systems

Phase diagrams for quaternary and higher order systems can be constructed as Jänecke[56] projections. The Jänecke plots for the following quaternary systems were made automatically using the Extended UNIQUAC model software. The same diagrams can be created by Aspen Plus or the OLI Stream Analyzer manually.

Phase diagrams for quaternary systems are three dimensional. Saturation surfaces in a three dimensional diagram mark an area in which a certain salt is saturated. Lines in the diagram mark compositions of solutions in equilibrium with two solid phases. The points where lines intersect mark compositions of solutions in equilibrium with three salts. An invariant point in a quaternary system marks the composition of a solution in equilibrium with four solid phases. A Jänecke plot is a projection of the three dimensional plot onto a two-dimensional surface. In this projection, the water content is not shown on a separate axis but can be plotted as contour lines—or as it is done here, as mass percent water in the diagram grid intersections. The two axes in a Jänecke diagram indicate the relative amounts of the two anions and the relative amounts of the two cations respectively. Here, the relative amounts are given as charge fractions. The charge of an ion is defined as the number of moles of the ion in 1 kg water multiplied with its charge number. The charge fraction is the charge of the anion or cation divided with the total charge of anions or cations in 1 kg water.

The selected data points used in the following calculations were all determined experimentally to be saturated with NaCl and one or two additional salts. The solubility of NaCl in the various solutions was calculated with the three different models and plotted in parity plots such as the one in Figure 8. The parity plots are used for comparing model calculations with the experimental data. The experimental data chosen for this comparison are located on the border lines of the NaCl fields in the Jänecke plots. In the case of the NaCl-

Table 8. Results of the Model Comparison for the Aqueous Na^+-Mg^{2+}-Cl^--SO_4^{2-} System at 35°C

	Experimental NaCl solubility (mol/kg H_2O)					Calculated NaCl solubility (mol/kg H_2O)		
No.	$MgCl_2$	$MgSO_4$	Na_2SO_4	NaCl	Solid Phases*	ElecNRTL optimized NaCl	OLI MSE NaCl	Extended UNIQUAC NaCl
I	5.88	0.050		0.075	1,2	0.16	0.119	0.34
II	5.89	0.049		0.075	1,2	0.16	0.118	0.34
III	3.68	0.661		0.494	2	0.52	0.65 [2]	0.93
IV	4.09	0.419		0.373	2	0.43	0.479 [2]	0.77
V	4.36	0.312		0.302	2	0.38	0.39 [2]	0.68
VI	5.47	0.089		0.109	2	0.2	0.163 [2]	0.4
VII	3.55	0.853		0.546	4	0.52	0.706 [2]	0.95
VIII	3.55	0.860		0.544	2,4	0.52	0.708 [2]	0.96
IX	3.01	1.03		0.866	4,5	0.74	0.943 [2,4]	1.44 [5]
X		0.279	0.441	5.59	6	6.07 [6]	5.69 [6]	5.69 [6]
XI		0.682	0.180	5.48	6	6.13 [6]	5.66 [6]	5.64 [6]
XII		0.850	0.080	5.42	6	6.16 [6]	5.65 [6]	5.62 [6]
XIII		0.944	0.044	5.38	5,6	6.17 [6]	5.64 [6]	5.61 [6]
XIV		0.945	0.047	5.36	5,6	6.17 [6]	5.64 [6]	5.61 [6]
XV	0.229	0.925		4.99	5	5.73 [6]	5.17 [6]	5.12
XVI	0.503	0.888		4.52	5	5.22 [6]	4.6 [6]	4.67 [5]
XVII	1.065	0.846		3.52	5	4.2 [6]	3.5	3.79 [5]
XVIII	1.64	0.854		2.58	5	3.24 [6]	2.55	2.96 [5]
XIX	2.18	0.884		1.78	5	2.37 [6]	1.77	2.26 [5]
XX	2.83	0.969		0.965	5	1.03 [6]	1.04 [4]	1.59 [5]
Average numerical difference						0.38	0.12	0.32

Experimental and calculated values of the solubility of NaCl in quaternary solutions. The experimental data are form Autenrieth and Braune.[41,47] The experimentally determined solid phases are given in column six. The solid phases determined by the models are given in brackets after the solubility. The roman numerals refer to the location of the experimental data in Figure 12. Solid phases in addition to NaCl are identified by 1 = $MgCl_2 \cdot 6H_2O$, 2 = $MgSO_4 \cdot H_2O$, 3 = $MgSO_4 \cdot 4H_2O$, 4 = $MgSO_4 \cdot 6H_2O$, 5 = $Na_2SO_4 \cdot MgSO_4 \cdot 4H_2O$, 6 = Na_2SO_4.

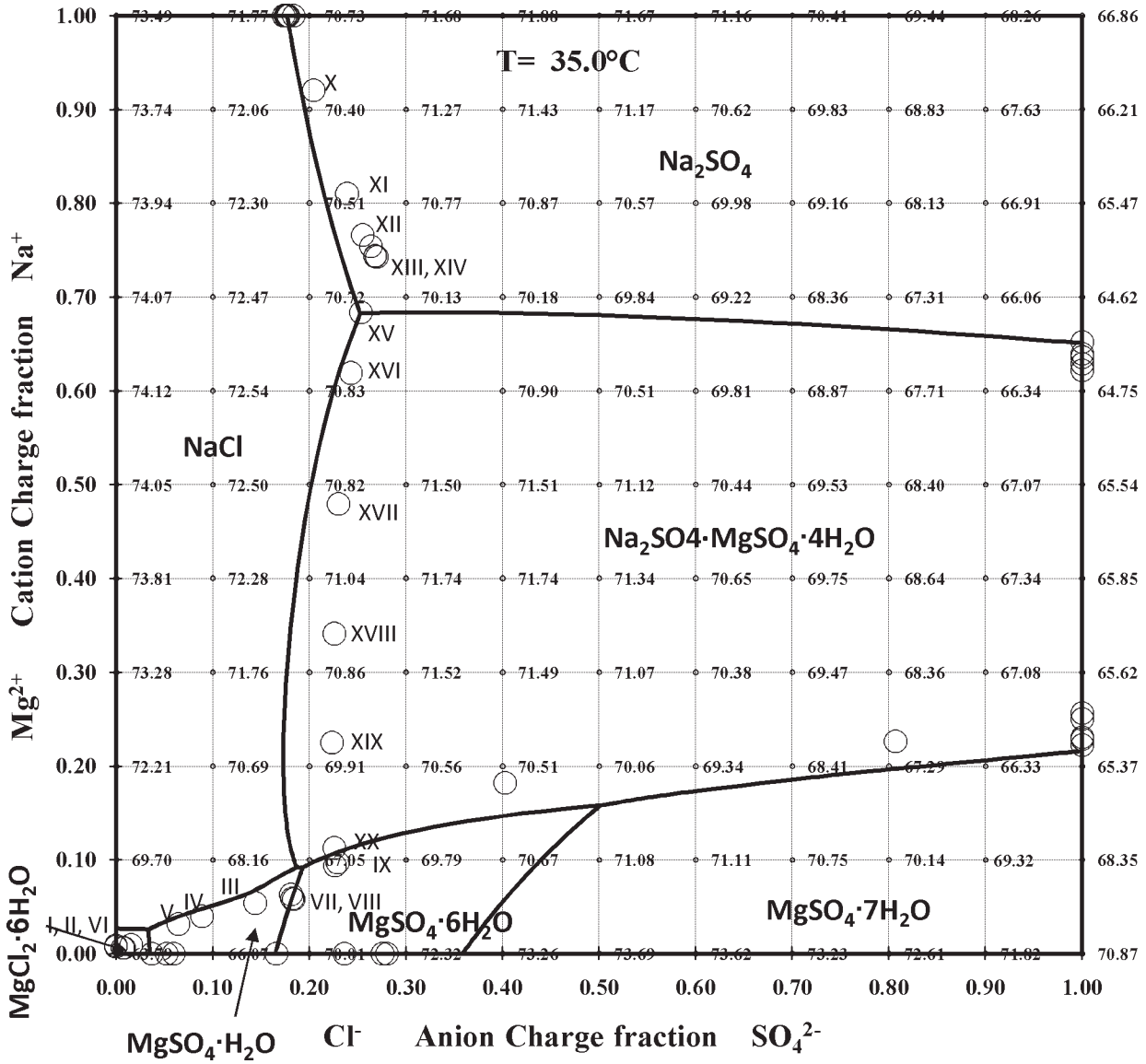

Figure 12. Quaternary phase diagram for the aqueous Na-Mg-Cl-SO_4 system at 35°C.

The solid line is the prediction by Extended UNIQUAC. The water content predicted by the Extended UNIQUAC model is given in mass percent at grid intersections in the diagram. The experimental data are mainly form Autenrieth and Braune.[41,47]

KCl-$NaNO_3$-KNO_3-H_2O system, test system IV in Figure 9, the NaCl field is the field in the upper left corner. The experimental data chosen for this comparison are marked with roman numerals in Figure 9.

The solid phases in equilibrium with the selected solutions are reported in the following tables together with the compositions of these solutions. The solid phases determined by the three thermodynamic models are also reported in tables. In most cases, there are differences between the experimentally determined solid phases and the solid phases determined by the models. An experimental point with three solid phases in equilibrium with the same liquid is a univariant point in a quaternary system. It can't be expected that any model would predict exactly the same three solid phases at the given temperature and composition. We seek to determine the solubility of NaCl in these solutions. The models will, therefore, invariantly find the points to be saturated with NaCl and perhaps with one more salt. If a model reports the precipitation of a solid that was not found to precipitate experimentally under the given circumstances it indicates an inaccuracy in the model.

Test System D: Na-K-Cl-NO_3-H_2O at 25°C

The solubility of NaCl in solutions containing various amounts of KCl, $NaNO_3$ and KNO_3 were calculated by the three different models. The experimental and calculated solubilities are presented in Table 6. The experimentally determined solid phases and the solid phases predicted by each of the three models are also given in Table 6. A parity plot showing the calculated solubility of NaCl versus the experimental solubility of NaCl is shown in Figure 8. Figure 9 is a Jänecke plot representing the phase diagram of the entire

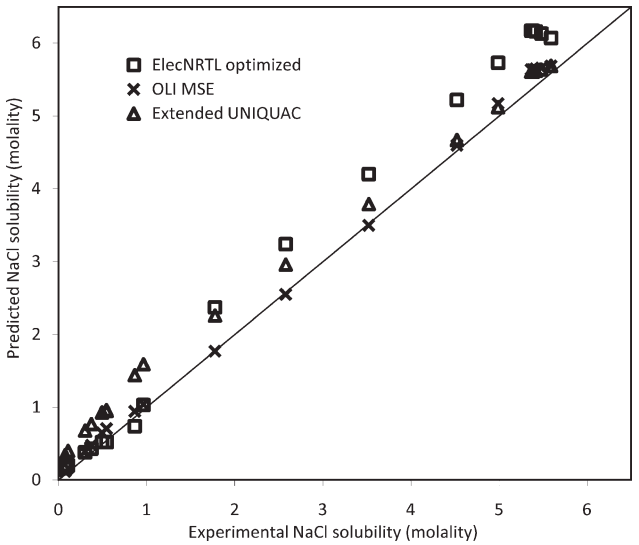

Figure 13. Parity plot for the NaCl solubility in the aqueous Na-Mg-Cl-SO_4 system at 35°C.

The experimental data are form Autenrieth and Braune.[41,47]

system. The visual impression from the phase diagram in Figure 9 is that the Extended UNIQUAC model gives the best results. According to Figure 8, the differences between the calculated NaCl solubilities are small in spite of the visual differences.

Test System E: Na-K-Cl-SO_4- H_2O at 20°C

The experimental and calculated solubilities of NaCl in solutions containing KCl, K_2SO_4, and Na_2SO_4 are shown in Table 7. The experimental data come from Teeple[45] and from Bergman and Rustamov.[46] The Jänecke plot for this quaternary system generated with the Extended UNIQUAC model is shown in Figure 10 together with the experimental data. The eleven experimental points saturated with NaCl chosen for comparing the models are marked with roman numerals in Figure 10. Some of these points look like they are identical in the Jänecke projection. There are, however, small differences in concentrations between the points, even between the points VII, VIII, IX, and X.

A parity plot comparing solubilities predicted with the three different models is shown in Figure 11. From this figure it is seen that the OLI MSE and the Extended UNIQUAC model give results of similar and reasonable quality while the calculations by "ElecNRTL optimized" deviate significantly from the experimental data. According to calculations with the ElecNRTL optimized parameters, Na_2SO_4 precipitates in all the considered experimental points I to XI in Figure 10. Actually, Na_2SO_4 was not supposed to precipitate in seven of these solutions according to the experimental phase diagram data. The Extended UNIQUAC model reports glaserite, $NaK_3(SO_4)_2$ to be precipitating for one of the solutions, composition X, where it was not supposed to precipitate. From Figure 10 it appears that the error is very small, because this experimental point is very close to the NaCl-$NaK_3(SO_4)_2$ line in the diagram.

Calculations carried out using the incomplete, built in parameters in the ElecNRTL model in AspenPlus result in significantly better agreement with the experimental concentrations than using the optimized ElecNRTL parameters. According to the calculations performed with the built in ElecNRTL parameters, $Na_2SO_4 \cdot 10H_2O$ is precipitating in the experimental points VI to XI in Figure 10. According to the experimental phase diagram this salt should not precipitate in any of these points.

Test System F: Na-Mg -Cl-SO_4- H_2O at 35°C

The calculated solubilities of NaCl in solutions containing $MgCl_2$, $MgSO_4$, and Na_2SO_4 are given in Table 8 together with experimental data from Autenrieth and Braune.[41,47] The Jänecke plot for this quaternary system generated with the Extended UNIQUAC model is shown in Figure 12 together with the experimental data. A parity plot comparing solubilities calculated with the three models is shown in Figure 13. According to Figure 13, the three models give results of similar and reasonable quality for this system. According to

Table 9. Results of the Model Comparison

	Experimental NaCl solubility (mol/kg H_2O)					Calculated NaCl solubility (mol/kg H_2O)		
No.	$MgCl_2$	$NaNO_3$	$Mg(NO_3)_2$	NaCl	Solid Phases*	ElecNRTL optimized NaCl	OLI MSE NaCl	Extended UNIQUAC NaCl
I		0.858	2.02	4.93	1	5.95 [1]	4.45 [1]	4.89
II	0.611		2.16	3.83	1	4.93 [1]	3.5 [1]	4.09
III	2.19		1.99	1.64	1	2.3 [1]	1.31	2.02
IV	2.60		2.50	0.563	1,2	1.93 [1]	0.852 [1]	1.56
V	4.07		2.28	0.329	2	0.41	0.252	0.728
VI	4.48		2.11	0.310	2,3	0.32	0.189	0.6
VII	4.32		1.63	0.315	3	0.36	0.24	0.656
VIII	5.02		1.04	0.213	3	0.24	0.158	0.472
IX	5.48		0.562	0.228	3	0.18	0.124	0.387
Average numerical difference						0.48	0.21	0.35

Predicted and experimental values of the solubility of NaCl in quaternary solutions at 25°C. The experimental data are from Leimbach and Pfeiffenberger.[49] The experimentally determined solid phases are given in column six. The solid phases determined by the models are given in brackets after the solubility. The roman numerals refer to the location of the experimental data in Figure 14.
*Solid phases in addition to NaCl are identified by 1 = $NaNO_3$, 2 = $Mg(NO_3)_2 \cdot 6H_2O$, 3 = $MgCl_2 \cdot 6H_2O$.

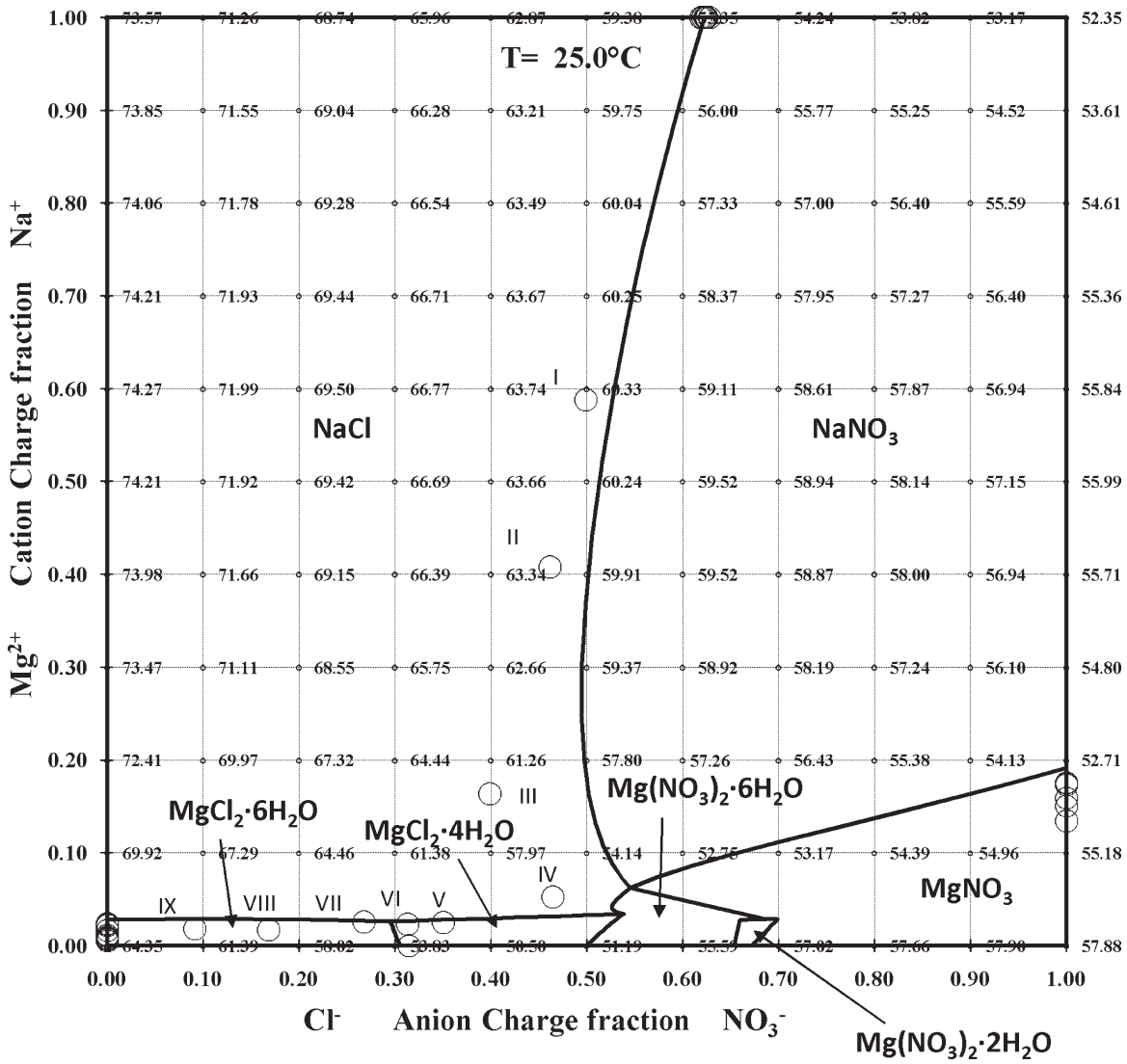

Figure 14. Quaternary phase diagram for the Na-Mg-Cl-NO_3 system at 25°C.

The solid line is the prediction by the Extended UNIQUAC. The water content calculated with the Extended UNIQUAC model is given in mass percent at grid intersections in the diagram. The experimental data are from Leimbach and Pfeiffenberger.[48]

Table 8, The OLI MSE model reports $MgSO_4 \cdot H_2O$ to be precipitating in one solution (IX) where it was not supposed to precipitate according to the experimental data. For two solutions (XV and XVI), the OLI MSE model predicts the precipitation of Na_2SO_4 and for one solution (XX) the precipitation of $MgSO_4 \cdot 6H_2O$ in contradiction with experimental data. These discrepancies are not serious but only indicate small differences from the experimental phase diagram. The ElecNRTL predicts the precipitation of Na_2SO_4 in six solutions (XV, XVI, XVII, XVIII, XIX, and XX) where it is not supposed to precipitate. This is a very serious discrepancy because it indicates that the ElecNRTL model with optimized parameters is not able to reproduce the area where bloedite, $Na_2SO_4 \cdot MgSO_4 \cdot 4H_2O$ is precipitating. This whole field in the phasediagram Figure 12 seems to be replaced with Na_2SO_4 by the ElecNRTL model. For the Extended UNIQUAC model, there are no disagreements between the calculated phases and the experimental phases for this system.

Test System G: Na-Mg-Cl-NO_3-H_2O at 25°C

The calculated solubilities of NaCl in solutions containing $MgCl_2$, $Mg(NO_3)_2$, and $NaNO_3$ are given in Table 9 together with experimental data from Leimbach and Pfeiffenberger.[48] The Jänecke plot for this quaternary system generated with the Extended UNIQUAC model is shown in Figure 14 together with the experimental data. A parity plot showing solubilities predicted with the three different models versus experimental data is shown in Figure 15. According to the parity plot, the OLI MSE and the Extended UNIQUAC models give results of similar and reasonable quality for this system. The ElecNRTL model with optimized parameters gives slightly larger deviations. All the models agree with the experimental data on the identity of the solid phases for this system.

Quinary systems

Test System H: Na-Mg-SO_4-Cl-NO_3- H_2O at 0°C The experimental data for the solubility of NaCl in solutions

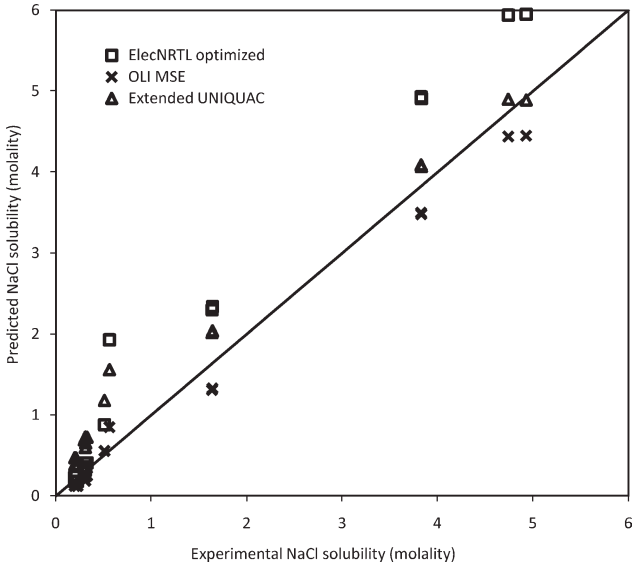

Figure 15. Parity plot for the calculated and experimental NaCl molality for the aqueous Na-Mg-Cl-NO_3 system at 25°C.

The experimental data are from Leimbach and Pfeiffenberger.[48]

containing $NaNO_3$, $MgCl_2$, $MgSO_4$, and $Mg(NO_3)_2$ are listed in Table 10 and includes the identity of the solid phases found experimentally. The experimental data are from Leimbach and Pfeiffenberger.[48] All the experimental solutions are saturated with NaCl and two or three additional salts. In the same table, the solubility of NaCl calculated with the three models is given along with the information on what solid phases each of the models found to be saturated in addition to NaCl. The parity plot of calculated versus experimental solubility of NaCl in this quinary system at 0°C is shown in Figure 16. According to the OLI MSE model kieserite, $MgSO_4 \cdot H_2O$ precipitates from two solutions rather than epsom salt $MgSO_4 \cdot 7H_2O$. At low temperatures the most hydrated salts are usually found to precipitate. This discrepancy could be related to the fact that the determination of parameters in the OLI MSE model is still a work in progress. The ElecNRTL model predicts the precipitation of $NaNO_3$ in one solution and the precipitation of $Na_2SO_4 \cdot 10H_2O$ in three solutions where these salts were not supposed to be saturated.

Test System I, NaCl-Mg SO_4-K_2SO_4-H_2O at 55°C

The experimental and calculated solubilities of NaCl at 55°C in solutions containing KCl, $MgCl_2$, $MgSO_4$, and K_2SO_4 are reported in Table 11. The Experimental data are from Janatjewa and Orlowa[49] (I to VIII) Kaskharov et al.[50] (IX to XVII), and Autenrieth[51] (data point XVIII). The solid phases found experimentally and by the programs are also given in Table 11.

The phase diagram for this quinary system was calculated with the Extended UNIQUAC model as shown in Figure 17a and b. All points in the diagrams are saturated with NaCl in addition to one or more salts. We have chosen to display the phase diagram as two separate diagrams of the Jänecke type. The NaCl content was not included in the calculation of the Jänecke coordinates.

The lines in these diagrams represent compositions of three salts in equilibrium with solutions. Each field in the diagram represents compositions of two salts (NaCl + one more salt) in equilibrium with solutions. In Figure 17a, the water contents of the saturated solutions are marked at the grid intersections, whereas in Figure 17b, the NaCl content is marked at the grid intersections. All the three-salt lines are identical in the two diagrams. A parity plot showing calculated versus experimental solubility data for this system is given in Figure 18.

In this system, the predictions of the OLI MSE and the Extended UNIQUAC models are of similar accuracy. The accuracy of the predictions made with the optimized ElecNRTL model is lower than for the other two models. The ElecNRTL found Na_2SO_4 to precipitate in five solutions (I, II, VII, VIII, XVIII) that are not supposed to be saturated with Na_2SO_4. According to Figure 17a and b, the composition of solution VIII is close to the experimental NaCl + Na_2SO_4 field. The other four solutions are far from the NaCl + Na_2SO_4 field. The same model found KCl to precipitate in five solutions (IV, V, VI, VII, and VIII) that are not supposed to be saturated with KCl. All these solutions are far from the NaCl + KCl field in Figure 17a and b. The OLI MSE model found glaserite, $NaK_3(SO_4)_2$ to precipitate in solution XVIII outside but near the NaCl + $NaK_3(SO_4)_2$ field. It also found $MgSO_4 \cdot H_2O$ to precipitate in two solutions

Table 10. Experimental and Calculated Values of the Solubility of NaCl in Quinary Solutions, mol/kg H_2O at 0°C

Experimental NaCl solubility (mol/kg H_2O)						ElecNRTL Optimized	OLI MSE	Extended UNIQUAC
NaCl	$NaNO_3$	$MgCl_2$	$MgSO_4$	$Mg(NO_3)_2$	Solid Phases*	NaCl	NaCl	NaCl
4.70	3.27		0.276	0.325	1,2	5.80 [1,2]	4.41 [2]	4.92
4.69	2.90		0.320	0.430	1,2	5.85 [1,2]	4.40 [2]	4.92 [2]
4.44		0.334	0.651	0.815	2,3	5.04 [1,2]	4.12 [2]	4.67 [2]
4.56	1.30		0.615	0.92	1,2,3	5.74 [1,2]	4.29 [2]	4.87 [2]
3.44		0.880	0.354	1.33	1,3	4.30 [1,2]	3.03 [1]	3.76
1.94		1.89	0.254	1.23	1,3	2.49 [1,2]	1.61 [1]	2.40
0.490		3.61	0.197	1.68	1,3,4	0.29	0.317 [6]	0.91
0.209		4.48	0.215	1.27	3,4,5	0.25	0.165 [6]	0.576
Average numerical deviation						0.71	0.27	0.32

The experimentally determined solid phases in equilibrium with the liquids are given in the sixth column. The solid phases determined by the models are given in brackets after the solubility. The experimental data are from Leimbach and Pfeiffenberger.[48]
*Solid phases in addition to NaCl are identified by 1 = $NaNO_3$, 2 = $Na_2SO_4 \cdot 10H_2O$, 3 = MgSO4·$7H_2O$, 4 = $Mg(NO_3)_2$ $6H_2O$, 5 = $MgCl_2 \cdot 6H_2O$, 6 = MgSO4·$7H_2O$

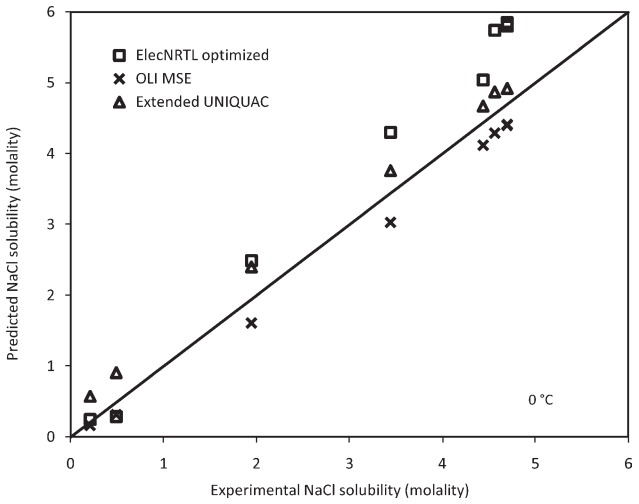

Figure 16. Parity plot for the predicted and experimental NaCl solubility in the aqueous Na-Mg-Cl-SO_4-NO_3 system at 0°C.

The experimental data are from Leimbach and Pfeiffenberger.[48]

(X and XI) and Na_2SO_4 to precipitate in solution (VIII) where these salts were not supposed to precipitate. The precipitation of $MgSO_4{\cdot}H_2O$ in solution X indicates some deviation from the experimental phase diagram. The Extended UNIQUAC model found glaserite, $NaK_3(SO_4)_2$ to precipitate in solution (XVIII) which is outside but near the NaCl + $NaK_3(SO_4)_2$ field in Figure 17a and b.

Mixed Solvent Electrolyte Test System J: NaCl-H_2O-C_2H_5OH (Ethanol) at 15 and 25°C

The performance of the three models for calculations in mixed solvent electrolyte solutions is illustrated in Figure 19 at 15°C and in Figure 20 at 25°C. For the mixed solvent electrolyte solution studied here, the Extended UNIQUAC model is giving the most accurate result. This must be seen in light of the particular way this model deals with mixed solvent solutions. The OLI MSE model and the ElecNRTL model both use the traditional mixed solvent approach, where standard state properties for electrolytes are functions of solvent composition.[9,11] In the Extended UNIQUAC model, the standard state for electrolytes and nonelectrolytes is the mole fraction based aqueous state, independent of composition. All deviation from ideal solution behavior is handled by the excess Gibbs energy function of the Extended UNIQUAC model. The influence of nonelectrolytes and electrolytes on the dielectric constant of water is ignored as it is assumed that ions mainly surround themselves with water rather than with nonelectrolytes.

The OLI MSE model is less accurate than the Extended UNIQUAC model in this test system. It was found that OLI's Zemaitis-Bromley aqueous model actually performed slightly better than the dedicated MSE model for this system. The reason for this seems to be the relative weighting of the SLE data used for determining parameters in the OLI MSE model. According to Anderko (Anderko A., Personal Communication, 2008), this will be solved in future versions of the program. The ElecNRTL model with optimized parameters performs slightly better than the ElecNRTL model with built in parameters.

Conclusion

Three activity coefficient models have been compared based on calculations done on 10 test systems all involving NaCl as one of the components. All three models are able to calculate vapour–liquid equilibrium reasonably well. It was found that the calculation of solid–liquid equilibria in multi component electrolyte solutions is a very difficult task. In most cases, but not in all, the models are able to calculate

Table 11. Experimental and Calculated Values of the Solubility of NaCl at 55°C in Quinary Solutions

	Experimental NaCl solubility (mol/kg H_2O)						Calculated NaCl solubility (mol/kg H_2O)		
	KCl	$MgCl_2$	$MgSO_4$	K_2SO_4	NaCl	Solid Phases*	ElecNRTL optimized NaCl	OLI MSE NaCl	Extended UNIQUAC NaCl
I	2.40	1.23	0.832		2.64	1, 6, 7	3.37 [2,6]	2.64 [1]	2.85 [1]
II	2.65	0.788	0.581		3.38	1, 6	3.87 [2,6]	3.35 [1]	3.49 [1]
III	3.01	0.131	0.325		4.49	1, 6	4.96 [6]	4.46 [1]	4.51 [1]
IV	1.18		1.05	0.150	5.01	1, 2, 8	5.55 [2,6]	5.31 [1,2]	5.20 [1,2]
V	1.18		0.919	0.169	5.03	1, 2	5.5 [2,6]	5.32 [1,2]	5.22 [1,2]
VI	1.00		0.686	0.278	5.35	1, 2	5.54 [2,6]	5.52 [1,2]	5.44 [1,2]
VII	1.74	0.777	1.09		3.38	1, 3, 7	4.17 [2,6]	3.36 [1]	3.56 [1,3]
VIII	1.61	0.192	1.16		4.38	1, 3, 8	5.05 [2,6]	4.46 [1,2]	4.46 [1,3]
IX	0.915	4.15	0.207		0.527	4, 6	0.54 [6]	0.52	0.83
X	1.39	2.93	0.569		1.15	4, 10	1.04 [6]	1.11 [5]	1.43 [4]
XI	0.749	2.95	0.689		0.923	4, 10	0.97 [6]	1.20 [5]	1.44
XII	0.412	3.82	0.605		0.541	4, 5, 10	0.54 [6]	0.689 [5]	0.95 [5]
XIII	1.61	2.66	0.511		1.34	4, 6	1.29 [6]	1.29	1.61 [4]
XIV	1.44	2.98	0.416		1.14	4, 6	1.09 [6]	1.09	1.41 [4]
XV	1.34	3.29	0.344		0.899	4, 6	0.91 [6]	0.905	1.22 [4]
XVI	1.20	3.59	0.278		0.722	4, 6	0.76 [6]	0.75	1.07
XVII	1.05	3.87	0.233		0.577	4, 6	0.64 [6]	0.624	0.934
XVIII	2.13	1.69	0.888		2.13	4, 6, 7	2.67 [2,5]	2.07 [1]	2.32 [1]
Average numerical deviation							0.29	0.09	0.24

*The solid phases are identified by: 1 = $NaK_3(SO_4)_2$, 2 = Na_2SO_4, 3= $Na_2SO_4{\cdot}MgSO_4{\cdot}4H_2O$, 4 = $KCl{\cdot}MgSO_4{\cdot}3H_2O$, 5 = $MgSO_4{\cdot}H_2O$, 6 = KCl, 7 = $K_2SO_4{\cdot}MgSO_4{\cdot}4H_2O$, 8 = $3Na_2SO_4{\cdot}MgSO_4$, 9 = $KCl{\cdot}MgCl_2{\cdot}6H_2O$, 10 = $K_2SO_4{\cdot}2MgSO_4$.

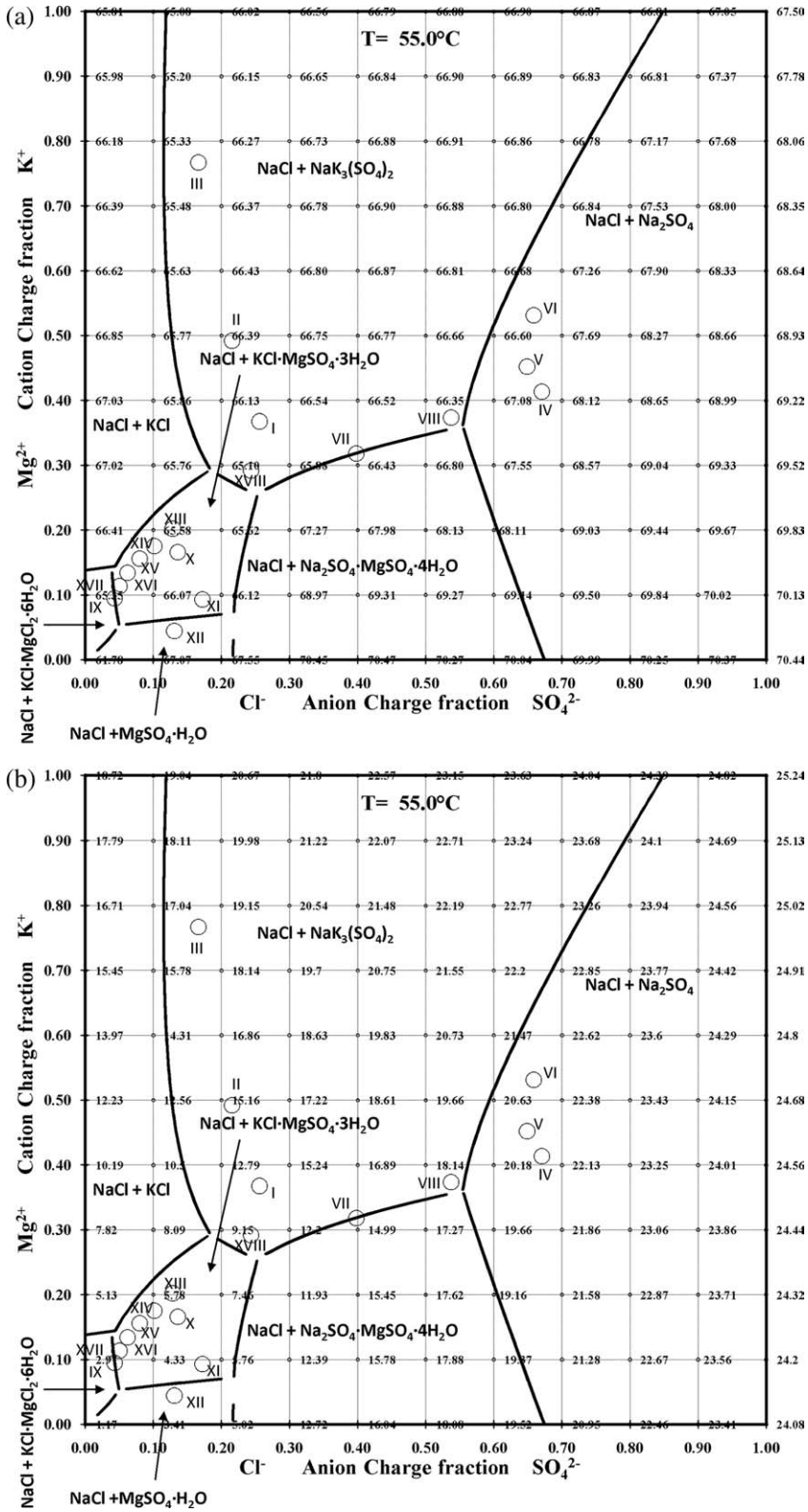

Figure 17. Quinary phase diagram for the NaCl-$MgSO_4$-K_2SO_4-H_2O system at 55°C. The solid line is the prediction by the Extended UNIQUAC model.

(a) The *water* content calculated with the Extended UNIQUAC model is given in mass percent at grid intersections in the diagram. The roman numerals refer to the experimental data in Table 11. (b) The *NaCl* content calculated with the Extended UNIQUAC model is given in mass percent at grid intersections in the diagram. The roman numerals refer to the experimental data in Table 11.

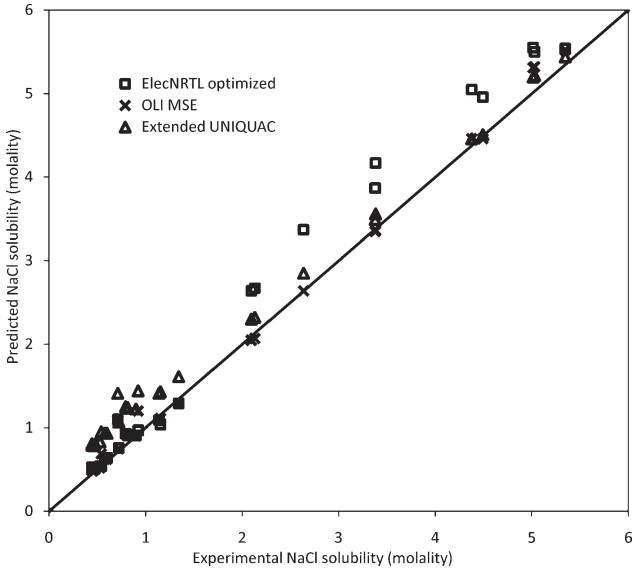

Figure 18. Parity plot for calculated and experimental NaCl solubility for the Na-Mg-Cl-SO_4-NO_3 system at 55°C.

The Experimental data are from Janatjewa and Orlowa,[49] Kaskharov et al.,[50] and Autenrieth.[51]

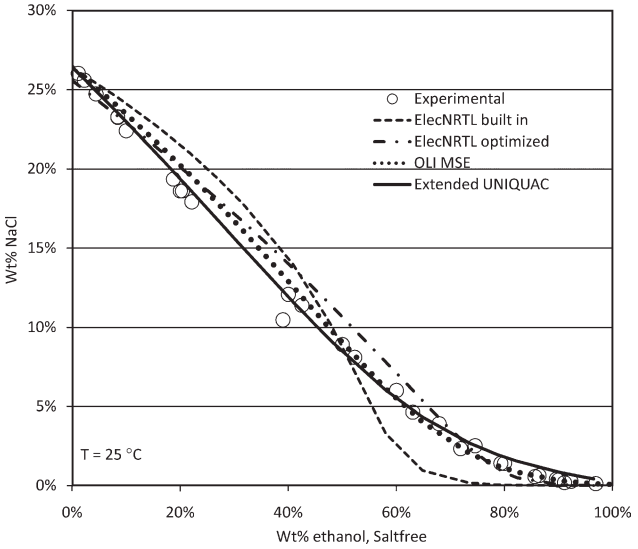

Figure 20. Solubility of NaCl in the mixed solvent H_2O-ethanol at 25°C as function of the ethanol wt % in the solvent on a salt-free basis.

Experimental data are from Krestov et al.,[52] Kopp,[54] and Armstrong et al.[55]

the concentrations at phase equilibrium with a reasonable accuracy. However, in most cases the models do not agree on the identity of the solids found at phase equilibrium and they do not agree with the experimentally found solid phases. It is problematic that irrespective of the model used, its applicability needs to be validated for the specific system and conditions you are working with.

The OLI MSE model and the ElecNRTL models are implemented in process simulators which make them useful for process simulation. The ElecNRTL model is built into the very open architecture of Aspen Plus, which allows the user to change the values of the model parameters based on the users own experimental data. The OLI MSE model is built into the OLI Stream analyzer which is very flexible and user friendly. A separate program, Regress, allows the user to change model parameters in the OLI MSE model. Determining new model parameters in an activity coefficient model is not a task for the common user but requires an expert.

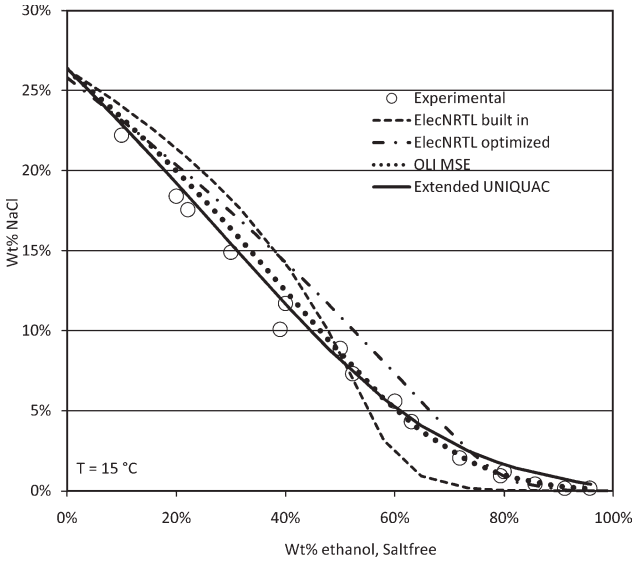

Figure 19. Solubility of NaCl in the mixed solvent H_2O-ethanol at 15°C as function of the ethanol wt % in the solvent on a salt-free basis.

Experimental data are from Krestov et al.[52] and Schiff.[53]

Acknowledgments

The authors would like to thank C.-C. Chen from Aspentech and A. Anderko from OLI Systems Inc. for their valuable comments to this work. We especially thank C.-C. Chen for preparing optimized parameters for the ElecNRTL model. These optimized parameters are available as Supporting Information from the website of the *AIChE Journal*.

Literature Cited

1. Meissner HP, Tester JW. Activity coefficients of strong electrolytes in aqueous solution. *Ind Eng Chem Process Des Dev*. 1972;11:128–133.
2. Meissner HP, Kusik CL. Activity coefficients of strong electrolytes in multicomponent aqueous solution. *AIChE J*. 1972;18:294–298.
3. Kusik CL, Meissner HP. Electrolyte activity coefficients in inorganic processing. *AIChE Symp Ser*. 1978;74:14–20.
4. Bromley LA. Thermodynamic properties of strong electrolytes in aqueous solutions. *AIChE J*. 1973;19:313–320.
5. Pitzer KS. Thermodynamics of electrolytes I. Theoretical basis and general equations. *J Phys Chem*. 1973;77:268–277.
6. Pitzer KS, Mayorga G. Thermodynamics of electrolytes. II. Activity and osmotic coefficients for strong electrolytes with one or both ions univalent. *J Phys Chem*. 1973;77:2300–2308.
7. Chen CC, Evans LB. A local composition model for the excess Gibbs energy of aqueous electrolyte systems. *AIChE J*. 1986;32: 444–454.
8. Chen CC, Britt HI, Boston JF, Evans LB. Local. composition model for excess Gibbs energy of electrolyte systems. *AIChE J*. 1982;28: 588–596.
9. Chen CC, Song Y. Generalized electrolyte-NRTL model for mixed-solvent electrolyte systems. *AIChE J*. 2004;50:1928–1941.
10. Wang P, Anderko A, Young RD. A speciation-based model for mixed-solvent electrolyte systems. *Fluid Phase Equilib*. 2002;203: 141–176.
11. Wang P. Anderko A, Springer RD, Young RD. Modeling phase equilibria and speciation in mixed-solvent electrolyte systems: II.

Liquid-liquid equilibria and properties of associating electrolyte solutions. *J Mol Liq.* 2006;125:37–44.
12. Kosinski JJ, Wang P, Springer RD, Anderko A. Modeling acid-base equilibria and phase behavior in mixed-solvent electrolyte systems. *Fluid Phase Equilib.* 2007;256:34–41.
13. Thomsen K, Rasmussen P, Gani R. Simulation and optimization of fractional crystallization processes. *Chem Eng Sci.* 1998;53:1551–1564.
14. Thomsen K, Rasmussen P. Modeling of vapor-liquid-solid equilibrium in gas-aqueous electrolyte systems. *Chem Eng.Sci.* 1999;54: 1787–1802.
15. Thomsen K. *Aqueous Electrolytes: Model Parameters and Process Simulation*. PhD thesis. Lyngby, Denmark: Technical University of Denmark, 1997.
16. Thomsen K. Modeling electrolyte solutions with the extended universal quasichemical (UNIQUAC) model. *Pure Appl Chem.* 2005; 77:531–542.
17. Chen CC, Britt HI, Boston JF, Evans LB. Two new activity coefficient models for the vapor-liquid equilibrium of electrolyte systems. In: Newman SA, editor. *Thermodynamics of Aqueous Systems with Industrial Applications. ACS Symposium Series 133*. Washington, DC, American Chemical Society 1980:61–89.
18. Austgen DM, Rochelle GT, Peng X, Chen CC. Model of vapor-liquid equilibria for aqueous acid gas-alkanolamine systems using the electrolyte-NRTL equation. *Ind Eng Chem Res.* 1989;28:1060–1073.
19. Chen CC. Representation of solid-liquid equilibrium of aqueous electrolyte systems with the electrolyte NRTL model. *Fluid Phase Equilib.* 1986;27:457–474.
20. Mock B, Evans LB, Chen CC. Thermodynamic representation of phase equilibria of mixed-solvent electrolyte systems. *AIChE J.* 1986;32:1655–1664.
21. Renon H, Prausnitz JM. Local compositions in thermodynamic excess functions for liquid mixtures. *AIChE J.* 1968;14:135–144.
22. Robinson RA, Stokes RH. *Electrolyte Solutions*. London: Butterworth, 1965.
23. Pitzer KS. Electrolytes from dilute solutions to fused salts. *J Am Chem Soc.* 1980;102:2902–6.
24. Zemaitis JF Jr. Predicting vapor-liquid-solid equilibria in multicomponent aqueous solutions of electrolytes. In: Newman SA, editor. *Thermodynamics of Aqueous Systems with Industrial Applications. ACS Symposium Series 133*. Washington, DC, American Chemical Society. 1980:227–246.
25. Gruszkiewicz MS, Palmer DA, Springer RD, Wang P, Anderko A. Phase behavior of aqueous Na-K-Mg-Ca-Cl-No_3 mixtures: isopiestic measurements and thermodynamic modeling. *J Solution Chem.* 2007;36:723–765.
26. Helgeson HC, Kirkham DH, Flowers GC. Theoretical prediction of the thermodynamic behavior of aqueous electrolytes at high pressures and temperatures: IV. Calculation of activity coefficients, osmotic coefficients, and apparent molal and standard and relative partial molal properties to 600°C and 5 kbar. *Am J Sci.* 1981;281: 1249–1516.
27. Fowler RH, Guggenheim AE. *Statistical Thermodynamics*. Cambridge, Cambridge University Press 1949.
28. Pereda S, Thomsen K, Rasmussen P. Vapor-liquid-solid equilibria of sulfur dioxide in aqueous electrolyte solutions. *Chem Eng Sci.* 2000;55:2663–2671.
29. Iliuta MC, Thomsen K, Rasmussen P. Extended UNIQUAC model for correlation and prediction of vapor-liquid-solid equilibria in aqueous salt systems containing non-electrolytes. Part A. Methanol-water-salt systems *Chem Eng Sci.* 2000;55:2673–2686.
30. Thomsen K, Iliuta MC, Rasmussen P. Extended UNIQUAC model for correlation and prediction of vapor-liquid-liquid-solid equilibria in aqueous salt systems containing non-electrolytes. Part B. Alcohol (ethanol, propanols, butanols)-water-salt systems. *Chem Eng Sci.* 2004;59:3631–3647.
31. Garcia AV, Thomsen K, Stenby EH. Prediction of mineral scale formation in geothermal and oilfield operations using the extended UNIQUAC model. Part I. Sulfate scaling minerals *Geothermics.* 2005;34:61–97.
32. Garcia AV, Thomsen K, Stenby EH. Prediction of mineral scale formation in geothermal and oilfield operations using the extended UNIQUAC model. *Geothermics.* 2006;35:239–284.
33. Wagman DD, Evans WH, Parker VB, Schumm RH, Halow I, Bailey SM, Churney KL, Nutall RL. The NBS tables of chemical thermodynamic properties. *J Phys Chem.* 1982;11 (Suppl 2); Ref Data.
34. Osokoreva NA, Opuikhtina MA, Shoikhet DN, Plaksina EF, Zaslavskii AI. Equilibria of the solutions in the system NaCl-KCl-$MgCl_2$-H_2O. *Tr Gos Inst Prikl Khim.* 1932;16:24–47.
35. Palkin AP. Solubility study in the system KCl-NaCl-$MgCl_2$-H_2O at temperatures below 10°. *Solikamskii Karnallity.* 1935;66–87.
36. Yanat'eva OK. Solubility polytherms in the systems CaCl2-$MgCl_2$-H_2O and $CaCl_2$-NaCl-H_2O. *Zh Prikl Khim.* 1946;19:709–722.
37. Liu CT, Lindsay WT Jr. Thermodynamic properties of aqueous solutions at high temperatures, US Office Saline Water. *Res Develop Progr Rep.* 1971;722:124.
38. Gibbard HF, Scatchard G, Rousseau RA, Creek JL. Liquid-vapor equilibrium of aqueous sodium chloride from 298 to 373K and from 1 to 6 mol/kg, and related properties. *J Chem Eng Data.* 1974;19:281–288.
39. Hakuta T, Goto T, Ishizaka S. Boiling point elevation of aqueous solutions containing inorganic salts. *Nippon Kaisui Gakkai-Shi.* 1974;28:151–155.
40. Robinson RA, Wilson JM, Stokes RH. The activity coefficients of lithium, sodium and potassium sulfate and sodium thiosulfate at 25°C from isopiestic measurements. *J Am Chem Soc.* 1941;63:1011–1013.
41. Autenrieth H, Braune G. Lösungsgleichgewichte des reziproken NaCl+$MgSO_4$+H_2O System. *Kali und Steinsalz.* 1960;3:15–30.
42. Reinders W. The reciprocal salt pair KCl + NaNO3 <–> NaCl + KNO3 and the manufacture of conversion saltpeter. *Z Anorg Chem.* 1915;93:202–212.
43. Cornec E, Krombach H. The study of equilibria between water, the nitrates, chlorides, and sulfates of sodium and potassium. *Annali di Chimica Applicata.* 1929;12:203–295.
44. Uyeda K. On the equilibrium of the reciprocal Salt Pairs: KCl + $NaNO_3$ <–> KNO3 + NaCl. *Mem College of Sci Kyoto, Imp Univ.* 1909–1910;2:249-250.
45. Teeple JE. *The Industrial Development of Searles Lake Brines*. New York: Academic press, 1929.
46. Bergman AG, Rustamov PG. Isotherms at 20, 25, and 30° of the reciprocal systems of chlorides and sulfates of sodium and potassium in water. *Zh Neorgan Khim.* 1958;3:2192–2199.
47. Autenrieth H, Braune G. The stable and unstable regions of the reciprocal salt pairs NaCl + $MgSO_4$ + H_2O in the case of saturation with NaCl. *Kali und Steinsalz.* 1960;3:85–97.
48. Leimbach G, Pfeiffenberger A. El sistema $NaNO_3$-Na_2SO_4-$MgCl_2$-H_2O en la zona de temperaturas de 0, 10, 25, 50, 75 y 100°C. *Caliche.* 1929;11:61–85.
49. Janatjewa OK, Orlowa WT. Über die Gleichgewichte im Meerwassersystem K, Na, Mg / Cl, SO4 - H2O bei 55°C, *Freib Forschungsh Reihe A, Bergbau.* 1959;123:119–126.
50. Kaskharov OD, Pasev'yeva LM, Nuryagdiyev M. The solutions saturated relative to cainite in (Na^+, K^+, Mg^{+2}), (Cl^-, $SO4^{-2}$), H2O system at 55°C Izv Akad Nauk Turkm SSR, Ser Fiz-Tekh. *Khim Geol Nauk.* 1975;4:77–81.
51. Autenrieth H. Neue, für die Kalirohsalzverarbeitung wichtige Untersuchungen am quinären, NaCl-gesättigten System der Salze ozeanischer Salzablagerungen. *Kali und Steinsalz.* 1955;11:18–32.
52. Krestov GA, Ovchinnikova VD, Vorontsova TK. Influence of dissolved atmospheric gases on the solubility of sodium chloride in water and aqueous solutions of Ethanol. *Russ J Inorg Chem.* 1977;22:1251–1252.
53. Schiff H. Über das Lösungsvermögen des Wässerigen Weingeists. *Liebig's Ann.* 1861;118:362–372.
54. Kopp H. Über die löslichkeit des kochsalzes in wässrigem weingeist. *annalen der chemie* (Weinheim) 1841;40:206.
55. Armstrong HE, Eyre JV, Hussey AV, Paddison WP. Studies of the processes operative in solutions, Part II-V. *Philos Trans R Soc Lond Ser A* 1907;79:564–597.
56. Jänecke E. Über eine neue Darstellungsform der wässerigen Lösungen. *Z Anorg Chem.* 1906;51:132–157.

Manuscript received Nov. 26, 2008, and revision received July 16, 2009.